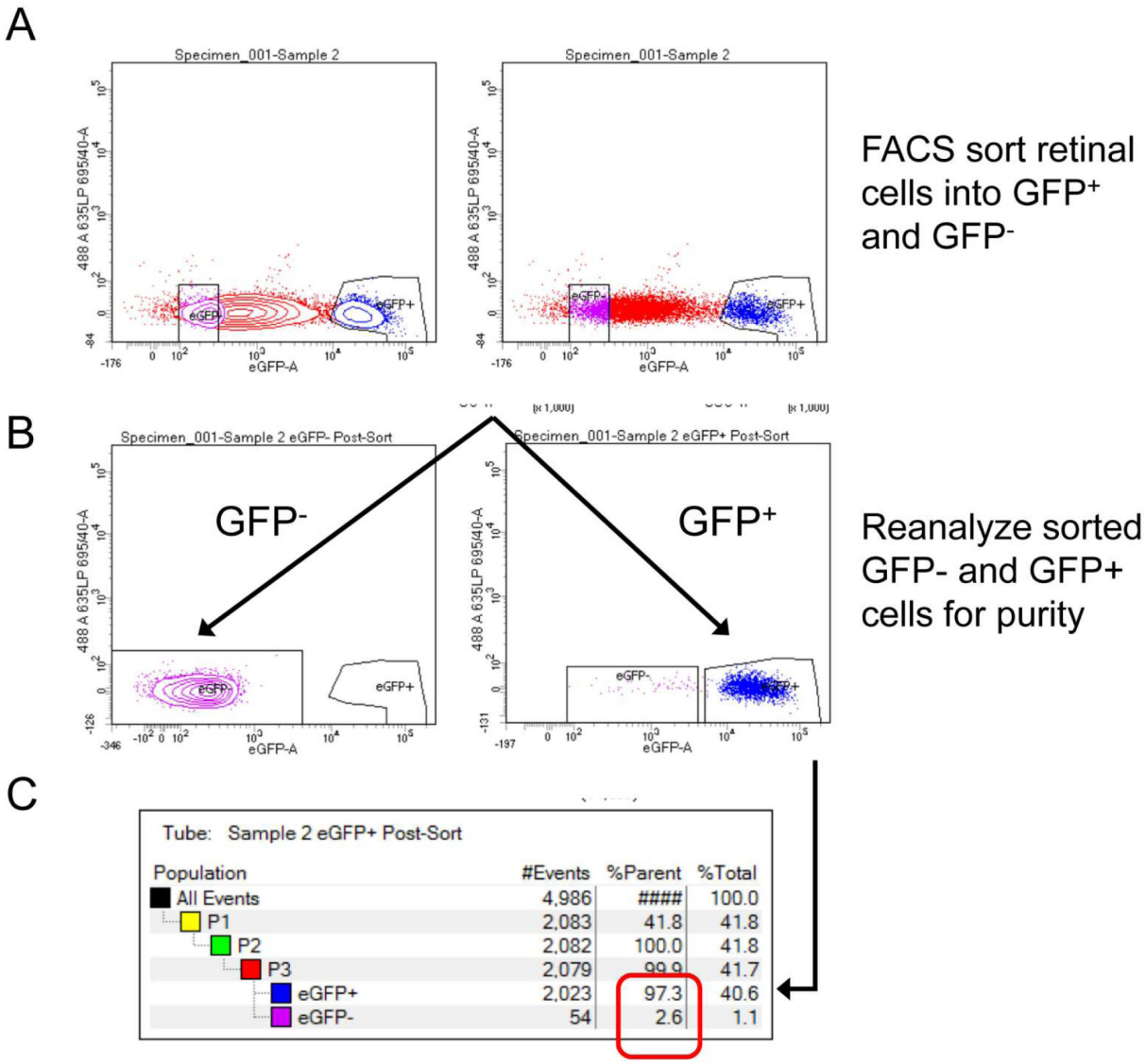

Figure S1. Verification of cellular purity for RNA isolation. The *Vsx2-Cre* driver used in these studies is fused to GFP, allowing us to collect CRE:GFP$^+$ retinal cells by flow cytometry. Retinae isolated from mice of the correct ages and genotypes were trypsinized into single cell mixtures. A. These were then sorted into GFP$^+$ and GFP$^-$ populations using fluorescence-activated cell sorting (FACS). B. GFP$^-$ and GFP$^+$ cell populations were retested for purity of GFP populations by flow cytometry. C. GFP$^+$ sorted samples were approximately 97% pure.

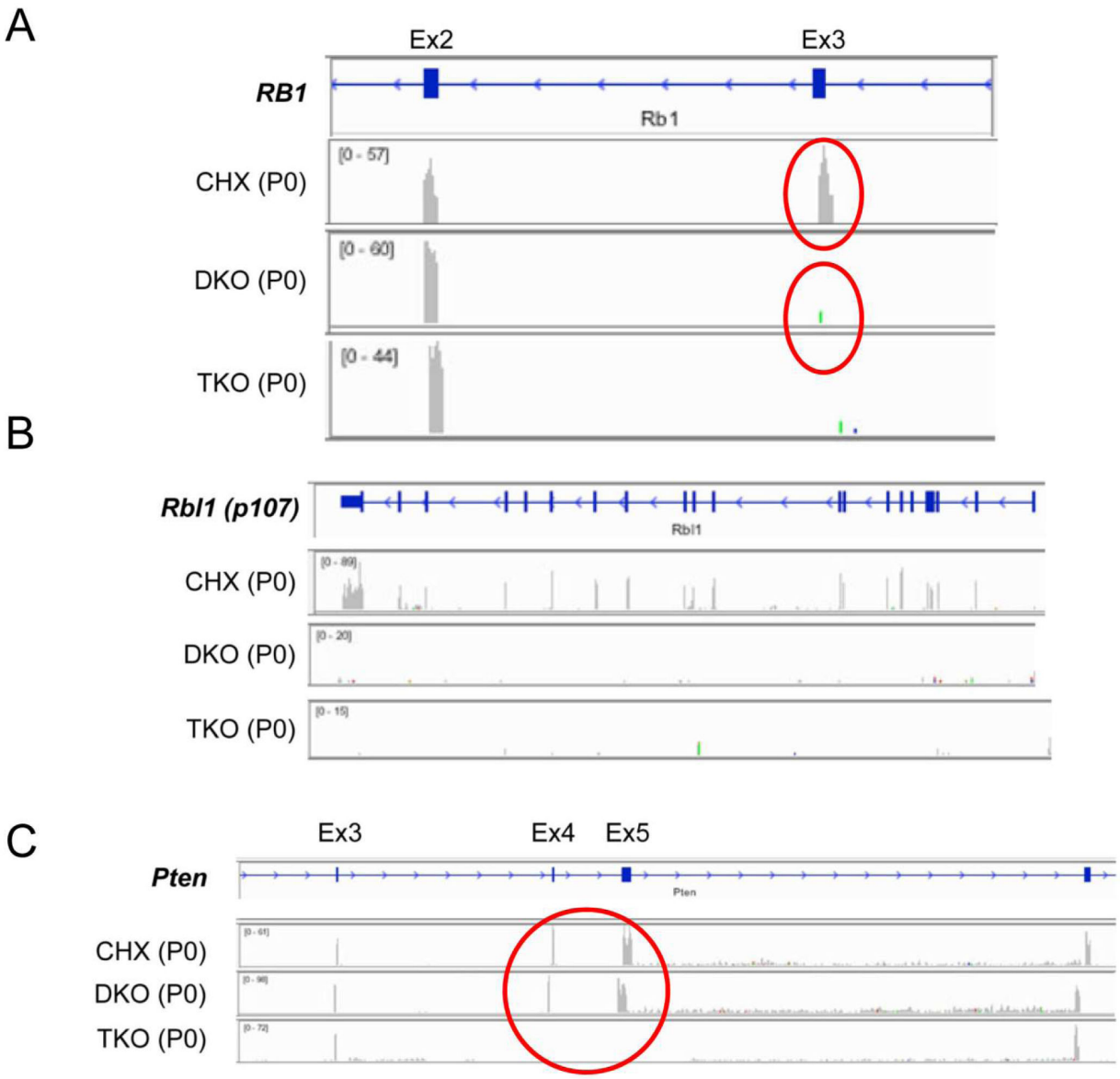

Figure S2. RNA-seq results were visualized using the Integrative Genomics Viewer (IGV). A. As expected, both *ΔRb/p107*- and *ΔRb/p107/Pten*-deficient retinae, but not control, shows loss of exon #3 of the Rb gene. B. Likewise, only ΔRb/p107- and *ΔRb/p107/Pten*-deficient samples lost tracks associated with the p107 gene, which is constitutively deleted in these retinae. C. Finally, only the *ΔRb/p107/Pten*-deficient retinae show loss of exons 4 and 5 of the *Pten* gene.

Cluster	Upstream Regulator	p-value		Gene Annotation	p-value
1 Progenitor	SMO	1.4E-09	1	positive regulation of cell proliferation	7.6E-05
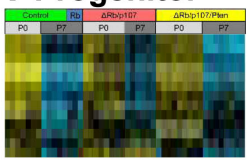	GLI3	1.1E-06	2	fibroblast growth factor receptor signaling	2.0E-04
	SHH	1.2E-06	3	regulation of muscle contraction	4.8E-04
	tretinoin	4.2E-06	4	ventricular cardiac tissue morphogenesis	8.7E-04
	CREB1	4.8E-06	5	multicellular organism development	3.9E-03
2 Cell Cycle					
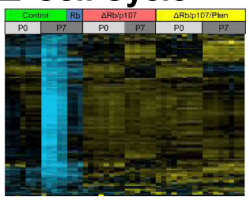	E2F4	2.0E-68	1	cell cycle	1.4E-87
	CDKN1A	7.8E-59	2	cell division	1.0E-60
	TP53	3.4E-49	3	mitotic nuclear division	1.3E-57
	dextran sulfate	2.0E-47	4	DNA replication	4.4E-39
	E2F1	5.8E-46	5	cellular response to DNA damage stimulus	5.0E-30
3 Immune					
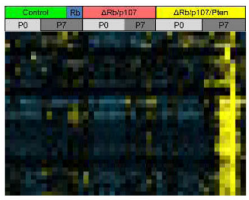	IFNG	4.1E-45	1	inflammatory response	4.7E-21
	lipopolysaccharide	4.3E-39	2	neutrophil chemotaxis	4.7E-14
	TGFB1	2.1E-28	3	immune response	6.8E-14
	IL10	1.2E-26	4	chemotaxis	2.1E-13
	IL6	1.1E-25	5	immune system process	6.4E-12
4 Mature	beta-estradiol	5.5E-12	1	cell adhesion	7.4E-06
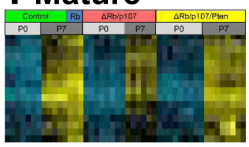	lipopolysaccharide	7.5E-10	2	inflammatory response	8.2E-05
	APP	8.5E-10	3	cell differentiation	2.1E-04
	IL1B	4.4E-09	4	nervous system development	2.1E-04
	Ifnar	8.5E-09	5	immune system process	2.5E-04
5 Differentiation					
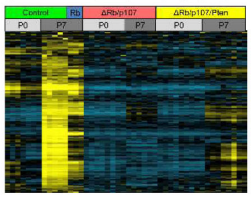	CRX	3.7E-21	1	visual perception	1.4E-37
	GNB3	9.2E-16	2	ion transport	1.3E-18
	REST	1.4E-13	3	response to stimulus	7.9E-17
	NRL	6.8E-12	4	homophilic cell adhesion plasma memb.	6.6E-15
	L-dopa	1.4E-11	5	regulation of ion transmembrane transport	2.0E-14

Figure S3. Ingenuity Pathway Analysis (IPA) of distinct gene expression clusters involved in cancer and development. Clusters from Figure 2 are shown at the left. Yellow cluster coloring represents high gene expression and blue indicates lower gene expression. We performed pathway and upstream regulator analyses using QIAGEN's Ingenuity® Pathway Analysis (IPA®, QIAGEN Redwood City, www.qiagen.com/ingenuity) tools and protein-protein interaction (PPI) network analysis. This software predicts upstream molecules, such as microRNA, transcription factors, or chemicals which cause similar gene expression changes elsewhere and thus may be causing the observed gene expression changes. Functional putative regulators and related functional gene annotation clusters identified using IPA are listed adjacent to the individual clusters, with the software calculated p-values.

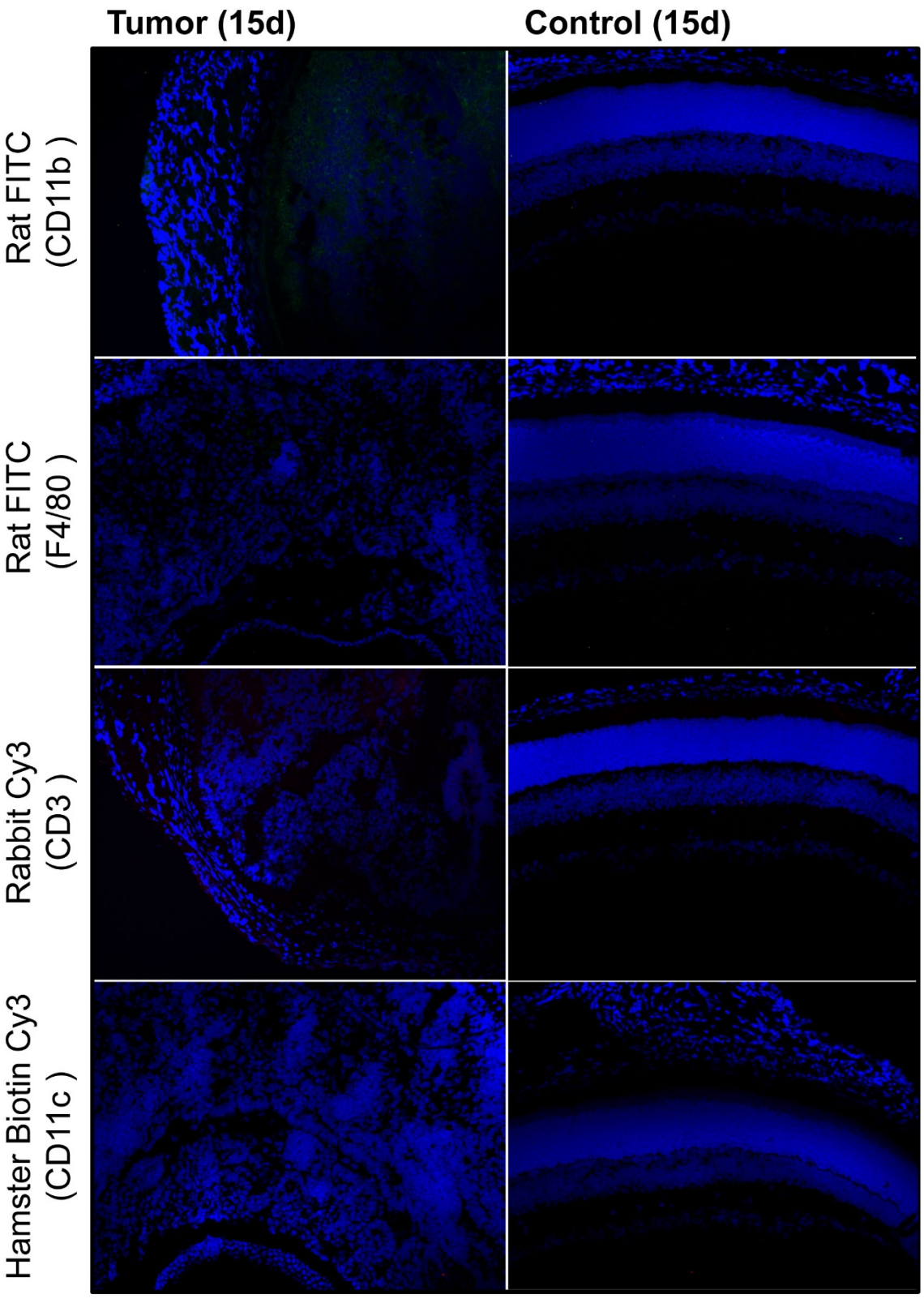

Figure S4. Control for immune cell staining in retinoblastoma tumors. Immunofluorescence (IF) staining performed at the same time as IF in Figure 3 but instead using isotype control antibodies for negative controls. IF was used to stain tumors and control retinae with rat FITC as control for CD11b and F4/80, Rabbit Cy3 as control for CD3, and Hamster biotin Cy3 as a control for CD11c. None of the isotype controls stained retinae.

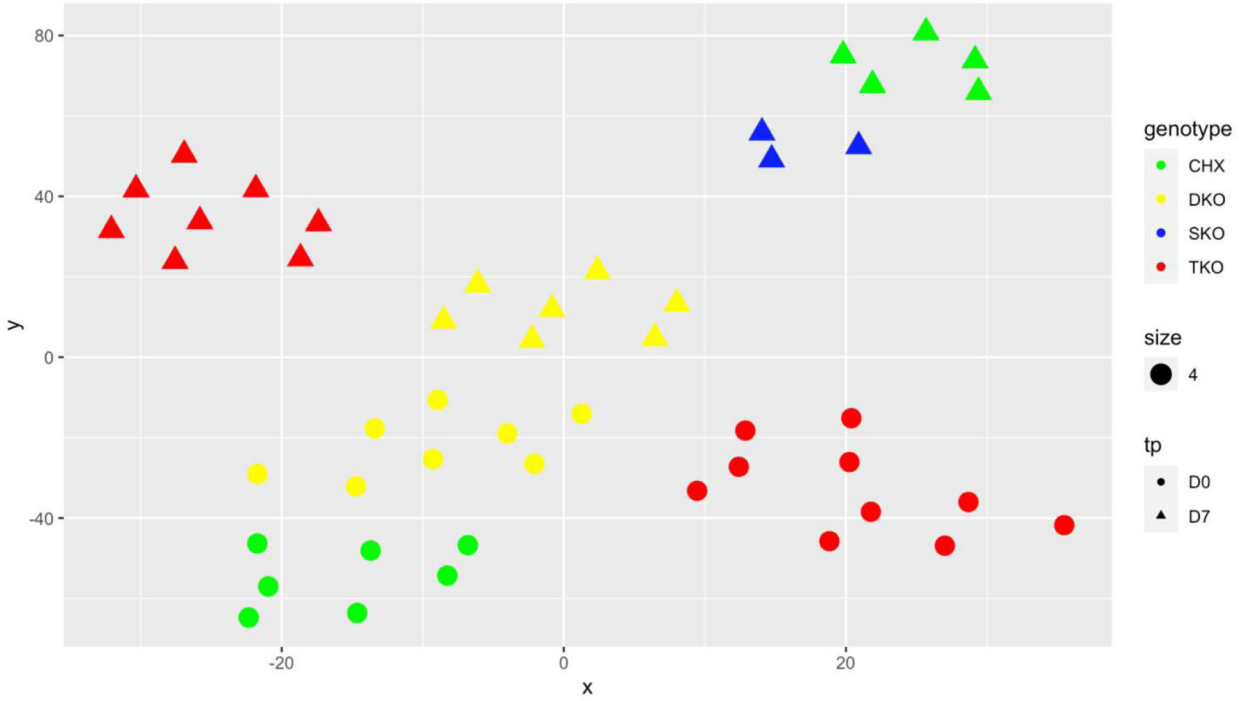

Figure S5. T-distributed Stochastic Neighbor Embedding (tSNE) analyses of RNA-Seq dataset. t-SNE is a machine learning algorithm for visualization. It is a nonlinear dimensionality reduction technique well-suited for embedding high-dimensional data for visualization in two-dimensional space. With perplexity=15, the resulting plot is highly consistent with the plot of the first two components using PCA, validating the work described in this paper.

Lane	Sample ID	Barcode	Reads
4	CHX-D0-1047739-1	ACAGTG	12150652
4	DKO-D0-1047823-8	ACTGAT	12988133
4	ΔRB-D7-1047745-1	ACTTGA	13171349
4	ΔRB-D7-1047745-8	AGTCAA	13043992
4	CHX-D7-1048043-1-3-4	AGTTCC	12521886
4	CHX-D0-1032030-1	ATCACG	12973662
4	CHX-D7-1048043-5-6	ATGTCA	12803485
4	DKO-D7-1047918-1	ATTCCT	12393865
4	CHX-D0-1047739-3	CAGATC	13160626
4	DKO-D0-1032037-1-2	CCGTCC	11288734
4	CHX-D0-1032030-2	CGATGT	12450858
4	DKO-D0-1047823-5	CGTACG	12020808
4	CHX-D7-1047745-7	CTTGTA	11843172
4	DKO-D0-1047823-7	GAGTGG	10744853
4	ΔRB-D7-1047745-3	GATCAG	11781254
4	CHX-D0-1047739-2	GCCAAT	12590000
4	CHX-D7-1047745-6	GGCTAC	12025952
4	DKO-D0-1032037-3	GTCCGC	11944213
4	DKO-D0-1047823-1	GTGAAA	12101587
4	DKO-D0-1047823-2	GTGGCC	12234106
4	DKO-D0-1047823-4	GTTTCG	12063745
4	CHX-D7-1047745-5	TAGCTT	12298944
4	CHX-D0-1032030-4-5	TGACCA	11867254
4	CHX-D0-1032030-3	TTAGGC	13079358
5	DKO-D7-1047823-4	ACAGTG	10675729
5	TKO-D7-1048011-6	ACTGAT	12414399
5	TKO-D0-1048083-7	ACTTGA	11739738
5	TKO-D0-1084380-2	AGTCAA	11201360
5	TKO-D0-1084380-3	AGTTCC	10311114
5	DKO-D7-1047918-2	ATCACG	11493094
5	TKO-D0-1084380-5	ATGTCA	10658386
5	TKO-D7-1048011-7	ATTCCT	12224427
5	TKO-D0-1048083-1	CAGATC	11611638
5	TKO-D0-1084380-9	CCGTCC	8532152
5	DKO-D7-1047920-1	CGATGT	10460359
5	TKO-D7-1048011-4	CGTACG	10787657
5	TKO-D0-1084380-1	CTTGTA	11469420
5	TKO-D7-1048011-5	GAGTGG	11336175
5	TKO-D0-1048037-2	GATCAG	11452360
5	DKO-D7-1047823-5	GCCAAT	11666984
5	TKO-D0-1084379-6	GGCTAC	11286522
5	TKO-D7-1048010-3	GTCCGC	13671353
5	TKO-D7-1048010-4	GTGAAA	11190269

5	TKO-D7-1048011-2	GTGGCC	11351036
5	TKO-D7-1048011-3	GTTTCG	10548612
5	TKO-D0-1048037-7	TAGCTT	10846032
5	DKO-D7-1047920-3	TGACCA	10864892

Table S1. Mapping statistics for RNA-sequencing reads per library by lane and barcode. This table contains detailed information regarding RNA-sequencing analysis, including the Sample ID, the sample barcode, and the total number of reads per sample.